Multifunctional Nanoparticles at the Hydrophilic and Hydrophobic Interface

Sangyeob Lee, Sheldon Q. Shi and H. Michael Barnes
Forest Products Department, Mississippi State University, Mississippi State, MS 39762, USA

Abstract

The objective of this study was to investigate a technique to obtain inorganic nanoparticle impregnated wood fiber reinforcement in the thermoplastic matrix. Inorganic nanoparticulates as a function of void filler and interfacial compatibilizer were generated through the chemically reconstruction method using two different ionic salts ($CaCl_2$ to Na_2CO_3). The longer reaction time of two ionic salts provided decreased nanoparticle sizes and uniform distribution. The increased molar ratios of $CaCl_2$ to Na_2CO_3 provided higher precipitation levels of $CaCO_3$. However, longer reaction times and higher ionic salt ratios resulted in a larger $CaCO_3$ crystal structure (>1 μm in diameter) which is not desirable because of 100 to 200 nm micropore sizes. SEM-EDX results also indicated Ca^{++} ion values observed in the cell wall of the fiber cross section. Reaction temperatures from 120 to 160°C and a concentration of 30% were the effective conditions, which provided a highest Ca^{++} ion value in the cell wall. The inorganic nanoparticle size and loading were controlled by different parameters of reaction time, temperature, molar ratio and moisture content. It should be noticed that the solid $CaCO_3$ crystal structure was relatively larger than chemically reconstruction nanoparticles on fiber surface. Furthermore, the reconstructed inorganic nanoparticles were more effective to be impregnated into the inner cellular structure.

Introduction

The cell wall structure of natural fibers contains many micropores. Also, some of the lignin and hemicellulose of natural fibers are usually removed during chemical treatments or pulping, which created additional micropores (Allan 1992). The presence of these micropores in the cell wall could cause manufacturing defects in composites, such as interfacial failure and air pockets. In order to reduce the air pocket defect, one can incorporate a vacuum assist system in the natural fiber polymer composite (NPC) processing to reduce the air bubble to some extent. Another efficient method is to introduce nano-particles into the micropores of the fiber cell wall structure through an impregnation process to fill those voids.

Compatibility between the hydrophilic natural fibers and the hydrophobic polyolefins has been a major issue for the NPC (Lee 2002, Ma *et al.* 2005). Lee *et al.* (2006) indicated that the deposited nano-scale particles on the natural fiber surface may serve as heterogeneous nucleation sites to initiate the crystalline orientation of the molten polymer

matrix. These results suggested that nanoparticles might control the heterogeneous nucleation of a semicrystalline polymer on the natural fiber surface. The natural fiber itself cannot initiate nuclei due to extremely unbalanced free energy between the cellulosic fibers and molten polyolefin matrices (Mullin 1993, Gasser *et al.* 2001, Lee *et al.* 2006). Therefore, the nanoparticle impregnation could not only fill the micro-pores of the fiber cell wall structure minimizing the air bubble defects of the NPC, but also introduce nanoparticles onto the fiber surfaces serving as attraction force manipulators to polymer matrixes to improve the compatibility at the fiber and polymer interfaces.

Calcium carbonate is a versatile additive for use in the pulp/paper and plastic industries for elastomeric applications to obtain a hydrophobic surface coating (Khrenov *et al.* 2005). It has a regular and controlled crystalline shape (orthorhombic) and a 0.05 to 2.5 μm particle size (Allan and Carroll 1994, Kuang *et al.* 2002, Yan *et al.* 2005). A smaller particle size can be achieved from ionic salt impregnation to build a crystal form of calcium carbonate (Choi 1995). Chemical impregnation technology has well been developed and applied in pulp and paper and surface coating industries (Allan *et al.* 1991, Allan *et al.* 1992a, b, Lee *et al.* 1999, Koepenick 2000, Lork 2004, Kuusipalo *et al.* 2005). However, in the pulp and paper applications, the amount of inorganic compound loading is limited to 7% due to the concerns of surface printing ability and paper strength (Kocman and Bruno 1995, Li *et al.* 2002, Perng and Wang 2004, Kralj *et al.* 2004, Frederick *et al.* 2004, Sancaktar and Walker 2004, Yan *et al.* 2005). For NPC applications, the amount of inorganic nanoparticle loading in the natural fibers can be increased, thus improving the attractive forces in the composites. The nanoparticle sizes and their distribution presented in the impregnated natural fibers may have a significant impact on the NPC properties. It has been shown that the inorganic nanoparticle size can be controlled by the reaction time and the ionic salt ratio (Choi 1995, Gasser *et al.* 2001).

The objective of this study was to develop inorganic nanoparticle impregnation techniques for the natural fiber cell wall structures in order to reduce the NPC processing defects and enhance the mechanical properties.

Experimental

Materials

In the inorganic nanoparticle impregnation experiments, Kraft wood pulp fibers (southern pine-*Pinus* spp.) were obtained from a local pulp company. They were collected from bleached pulp stream and kept wet condition (150% moisture content; MC) to obtain optimum nano-void openings. The fibers were stored at a temperature of 4 °C. Primary (Na_2CO_3) and secondary ionic ($CaCl_2$) salts were purchased from Fisher Scientific Inc.

Experimental Procedures

Nanoparticle Impregnation into Micropore Structures with Inorganic Nanoparticles

Fig. 1 shows a simplified flow chart for the inorganic nanoparticle impregnation using two steps of the ionic salt treatment under heated and pressurized chamber conditions. Micropore impregnation of ionic salts was processed with never-dried kraft pulp fibers in a

pressurized reactor. The primary salt, Na_2CO_3, and secondary ionic salt, $CaCl_2$, were impregnated into micropores of the pulp fiber cell wall consecutively to obtain nanoparticles (< 100 nm). The nanoparticale sizes were controlled by the reaction time and molar fraction of ionic salts. The chemical reaction is described as follows:

$$CaCl_2 \cdot H_2O + Na_2CO_3 \xrightarrow{H_2O} CaCO_3 + 2NaCl + 2H_2O$$

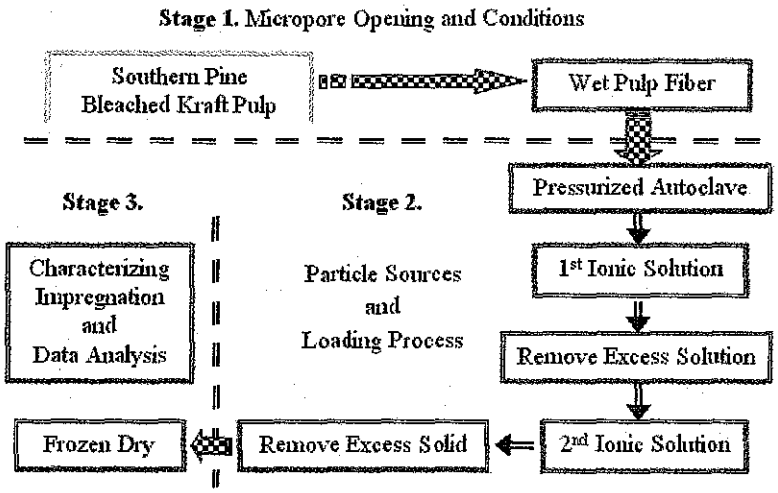

Fig 1. Inorganic Nanoparticle Impregnation using two steps of the ionic salt treatment under heated and pressurized chamber conditions.

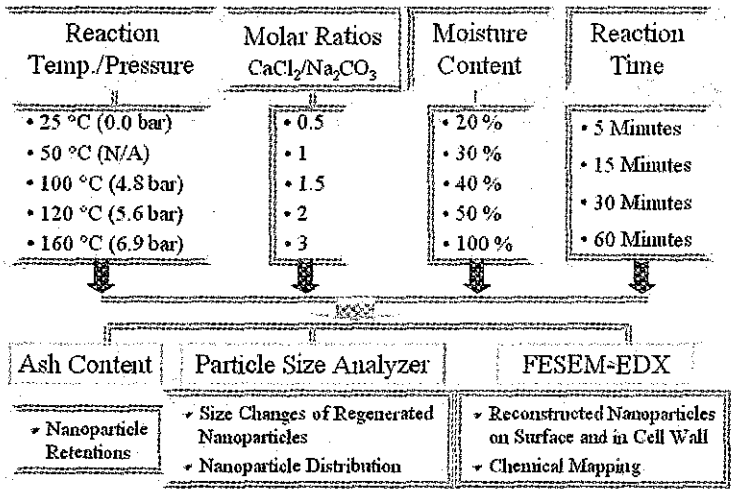

Fig. 2. Experimental variables for the inorganic nanoparticle impregnation into the cell wall structure of wood pulp fibers

For this study, parameters (Fig. 2) were selected to optimize inorganic nanoparticle loading into the porous structures of pulp fibers. The parameters investigated include reaction temperature, molar ratios of two ionic salts, moisture content (MC) of fibers, and reaction time. The experimental process was to optimize process to get the best impregnation conditions. The moisture contents (MC = oven-dry weight basis; ODB: 20, 30, 40, 50, 100%) with Molar Ratio (=1) to see the effect of MC. From the result, 20 and 30% of MC were selected. Molar Ratios (= 0.5, 1, 1.5, 2, and 3) with the two MC were evaluated by Ash contents of pulp fibers impregnated with $CaCO_3$. After previous steps, reaction temperature and time factors were preceded without kraft pulp with primary (Na_2CO_3) and secondary ionic salt ($CaCl_2$). Temperatures (25, 50, 100, 120 and 160 °C) were evaluated with a fixed molar ratio (=1) and MC (30%). The effect was evaluated with particle size analysis and SEM to address how the temperatures influence the nanoparticle formation and sizes. Two molar ratios (= 0.5 and 1), a MC (30%) and a temperature (25°C) were selected to evaluated reaction times (5, 15, 30 and 60 minutes) between primary and secondary ionic salts after primary ionic salt was diluted for 15 minutes. The selected parameters such as molar ratio (=1), a MC (30%), a temperature (25 and 160°C) and a reaction time (15 minute) were directly applied to impregnate nanoparticles into the cell wall structure of kenaf fibers. SEM-EDX was used to evaluate the Ca++ ion mapping and Chemical element analysis.

A 1-L pressurized reactor (Parr Instrumental Co.) with Model 4843 controller was employed to inorganic nanoparticle impregnation process. In a typical experiment, bleached commercial pulp fibers (0.5% ash content, 91% moisture content (ODB)) were introduced into the pressure vessel along with the primary ionic solution. The vessel was sealed and pressurized to the level shown in Fig. 2 for the reaction temperature used. The solution was constantly stirred at 100 rpm. Pressure was maintained for 15 minutes followed by venting to atmospheric pressure and removal of the reacted fiber. After washing out the excess primary solution, the fiber was reintroduced into the reaction vessel with the secondary ionic salt and the process repeated. The inorganic nanoparticle impregnated fibers were dried and evaluated in terms of nanoparticle size distribution, surface morphology, and chemical loading of the inner cell wall structure of the natural fibers. The treated fibers were freeze-dried under vacuum for 12 hours and stored in a vacuum desiccator. A muffle furnace was used to measure ash contents (TAPPI 1993) for each treatment condition.

A Particle Size Analyzer (Microtrac UPA 250) with Microtrac V.9.1.17 software was used to determine inorganic nanoparticle growth and distribution. The micro to nano scales of particles were detected by dynamic light scattering detector (0.003 to 6.541 micron capability) for 180 seconds. Nanoparticle samples were treated with sonic waves for three minutes to increase the detector sensitivity. Deionized water was used as a carrier. The morphology and chemical mapping analysis using field emission scanning electron microscopy (FESEM: JSM-6500F and EDX: Oxford Instruments INCA Energy with X-ray Elemental Analysis) were used to investigate the inorganic nanoparticle distribution in the cell wall and surface morphology. Mounted fibers were coated with an approximately 15-nm thin gold layer using an ion sputter. Images were generated at 5 kV and 10, 000x.

Results and Discussion

Effect of Reaction Temperature

Fig. 3 shows the effect of reaction temperature on the inorganic nanoparticle formation and growth in the reaction chamber. The nanoparticle sizes were from 138 nm to 2,000 nm. The crystal size was decreased with an increased reaction time. Also, the longer the reaction time, the more uniform for the particle size distribution. Nano-scale crystal formation on the surface of micro-scale inorganic particles was observed at a relatively lower temperature under 50 °C. When the reaction temperature reached 160 °C, the reaction chamber pressure was 6.9 bar, of which might play a role of inorganic nanoparticle formation and growth during the reaction of two ionic salts. Optimum reaction time was 15 minutes after the secondary ionic salt was introduced into the reaction chamber. The reaction time was evaluated at a temperature of 25 °C with two types of molar ratios of sodium carbonate and calcium chloride. The longer reaction time contributed to the growth of $CaCO_3$ crystal structures. The molar ratios of $CaCl_2/Na_2CO_3$ (= 1 and 2) provided relatively low average particle size. The ratio (= 2) showed a wide distribution from 45 nm to 6um, while the ratio (= 1) showed a relatively uniform distribution.

Moisture Content of Kraft Pulp

Fig. 4 shows the effect of fiber MC on the nanoparticle loading for the fiber cell wall impregnation. It shows that the fiber saturation point (FSP) of the bleached kraft fibers is a critical point to impregnate the fillers into their cell wall structure. Due to the MC changes

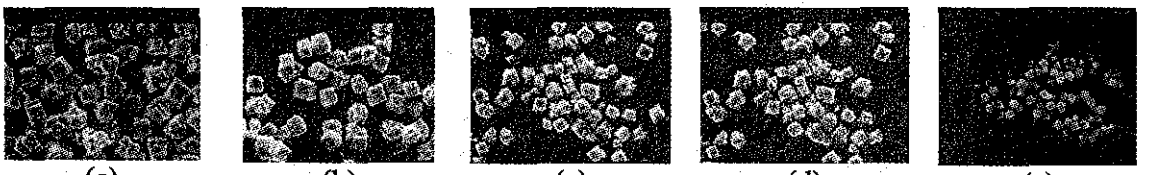

Fig. 3. Inorganic nanoparticle formation and growth of consecutively reacted ionic salts with reaction time applied in the reaction chamber at 2000 x. (a) 25 °C, (b) 50 °C, (c) 100 °C, (d) 120 °C, and (e) 160 °C

below FSP, cellular structures of natural fiber cell wall may play an important role. It also influences the dispersing characteristics of ionic salts into porous structure of the cell wall. Below FSP, the microfibrils are closer, and fewer micropores are available to be impregnated with inorganic fillers (Choi 1995, Kocman and Bruno 1996). It should also be noted that the dry fibers are not compatible with the impregnation of inorganic compounds due to the collapsing cellular structure of fiber cell walls. It is difficult to recover their structure with swelling agents (Allan 1992, Choi 1995). In this impregnation study, we targeted 10 to 15 % inorganic nanoparticle loading in order to keep both the fiber strength properties and the void filling requirement. Since the inorganic nanoparticle loading is higher than the target (10 to 15%), all of the wet fiber conditions can be acceptable for the nanoparticle loading except that the MC remains below FSP.

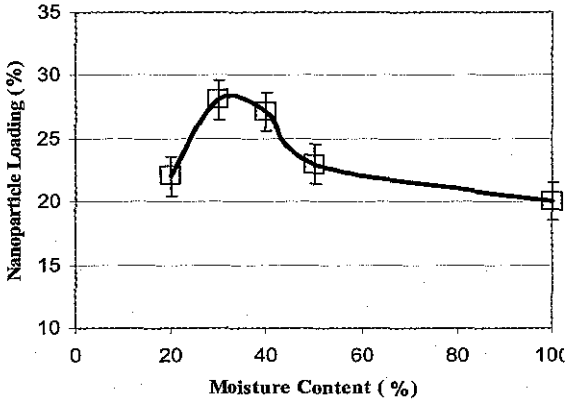

Fig. 4. Moisture contents of Kraft fiber on a wood cell wall loaded with CaCO3 particles.

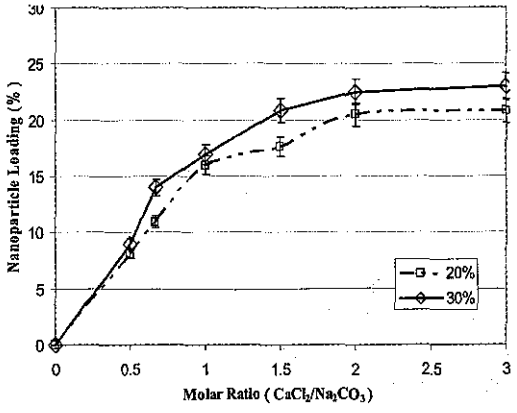

Fig. 5. The effects of molar ratios of calcium chloride and sodium carbonate on CWL of wood fibers at 25°C for 30 minutes.

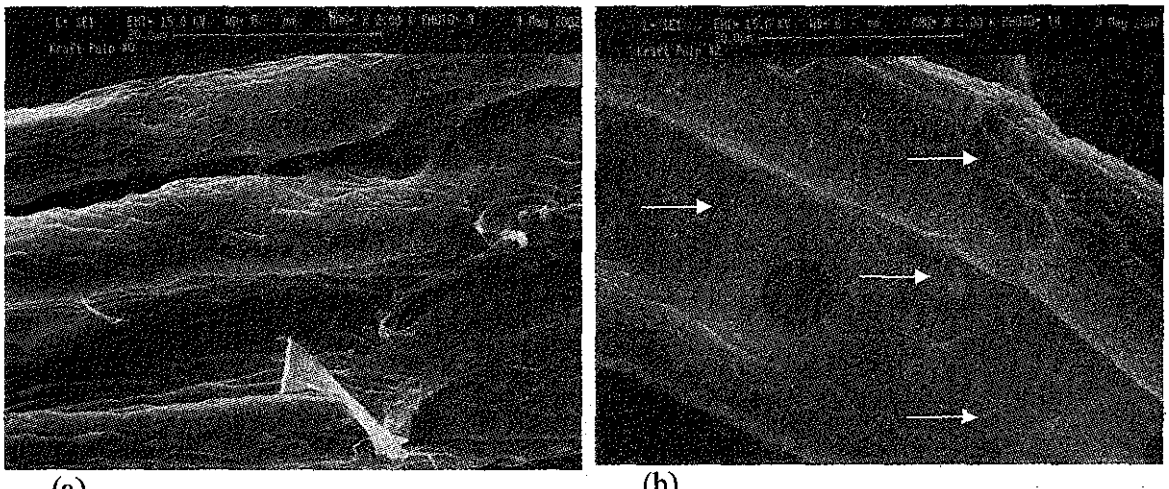

(a) (b)

Fig. 6. Surface nanoparticles formed by excessive ionic salts. (a) Before ionic treatment and (b) After ionic treatment.

Effect of Molar Ratios of Ionic Salts

Fig. 5 shows that a higher concentration of calcium chloride ($CaCl_2$) and a greater molar ratio (calcium chloride to sodium carbonate =$CaCl_2/Na_2CO_3$) are required to achieve a higher precipitation level of calcium carbonate ($CaCO_3$). Additional findings suggest that longer reaction times and higher ionic salt ratios will result in a large $CaCO_3$ crystal structure (up to > 1 μm in diameter). The desirable particle sizes for the nanoparticle impregnation are in the range of 10 nm up to 200 nm. This can be achieved by controlling the reaction time and calcium chloride contents in the ionic salt ratio. The effect of molar ratios ($CaCl_2/Na_2CO_3$ =1) of ionic salts addressed 16 % to 17% cell wall loading capability.

Reconstructed Nanoparticles and $CaCO_3$ Precipitation

Figs 6 and 7 show the FESEM images and the EDX analysis before and after inorganic nanoparticle impregnation. The morphological images show that the deposit materials remain on the surface. The deposited materials may consist of lignin and hemicellulose materials as well as the particles from natural fiber itself. The bright particles shown in Fig. 6b, indicate that the inorganic crystal is formed on the surface and grown with excessive ionic salts. The residual ionic salts generally allow forming larger crystals of the calcium carbonate than the crystals formed inner cell wall. Because the largest voids are generally around 100 nm, the inorganic nanoparticles loaded inner cell wall may be less than the largest voids. The evidence of calcium carbonate impregnation as a filler of the nano-scale porous structure in the natural fiber cell wall is shown in Fig. 7. The red dots (Fig. 7a) indicate Ca++ ion distribution inner cell wall structures. The dots also indicate that impregnated inorganic nanoparticles ($CaCO_3$) are uniformly distributed through the natural fiber cell wall. The energy dispersive x-ray analysis (Fig. 7b) shows higher quantities of Ca++ ions with residual sodium and chloride ions.

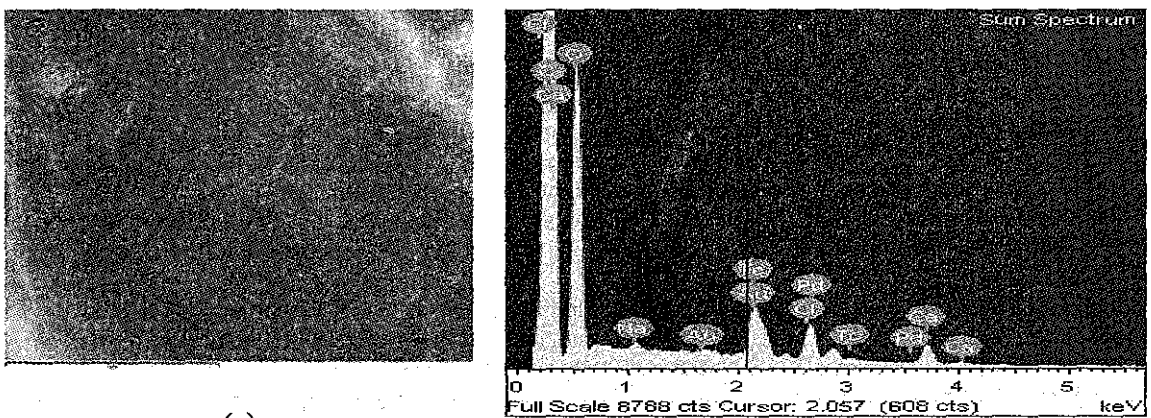

Fig. 7. Chemical mapping of Ca++ ion in cross section using SEM-EDX in the cell wall structure of natural fibers. (a) Ca++ ion mapping, and (b) Chemical element analysis.

Conclusions

Through the impregnation process developed in this study, inorganic nanoparticles were observed in the micropore structure of the cell wall. These nanoparticles may serve as void fillers and potentially provide nuclear sites for the semi-crystalline polymers. The longer the reaction time, the smaller the reconstructed nanoparticle size, and the more uniform nanoparticle size distribution obtained. Parameters for the inorganic nanoparticle impregnation using ionic salts to the natural fiber cell wall structures were evaluated to optimize the attraction force at the fiber and polyolefin interphase. The inorganic nanoparticle precipitation increased with an increase of $CaCl_2/Na_2CO_3$ molar ratios. The shorter the reaction time, and the higher the reaction temperatures (120 to 160°C) with applied pressure, the smaller the reconstructed nanoparticle size and the more uniform the

nanoparticle distribution obtained as optimum loading conditions. An optimum MC for the inorganic nanoparticle loading was at FSP. Under the optimum conditions, Ca++ ion values were observed in the cell wall of the fiber cross section. Through the developed impregnation process, the inorganic nanoparticles are observed in the micropore structure of the cell wall. These nanoparticles may serve as void fillers in the micropores of the natural fibers. Also, the nanoparticles may potentially provide nuclear sites for the semi-crystalline polymers.

Acknowledgment

The authors would like to express appreciation for the support of the US Department of Energy and the Center for Advanced Vehicular Systems at Mississippi State University. The authors would like to thank Dr. James Rawlins and his research group, Thames-Rawlins Polymer Research, Shelby Freland Thames Polymer Science Research Center, University of Southern Mississippi, Hattiesburg, MS for instrumental support.

References

Allan, G.G., Y.C. Ko, and P. Ritzenthaler. 1991. The microporosity of pulp. Tappi J. 74(3): 205.

Allan, G.G., A.R. Negri, and P. Ritzenthaler. 1992a. The microporosity of pulp; the properties of paper made from pulp fibers internally filled with calcium carbonate. Tappi J. 75(3):239-244.

Allan, G.G., J.P. Carroll, A.R. Negri, M. Raghuraman, P. Ritzenthaler, and A. Yahiaoui. 1992b. The microporosity of pulp; the precipitation of inorganic fillers within the micropores of the cell wall. Tappi J. 75(1):175-178.

Allan, G.G. 1992. Cell wall loading of never-dried pulp fibers. U.S. pat. 5,096,539 (Mar. 17, 1992).

Allan, G.G. and J.P. Carroll. 1994. Composition and methods for filling dried cellulosic fibers with an inorganic filler. U.S. pat. 5,275,699 (Jan. 4, 1994).

Choi Y.D. 1995. Impreagnation behavior of $CaCO_3$, KCl and K_2SO_4 into micropore of pulp fiber. MS thesis, Yeungnam Univ., Kyungsan, Korea. 41p.

Frederick, W.J., B. Shi, D.D. Euhus, and R.W. Rousseau. 2004. Crystallization and control of sodium salt scales in black liquor concentrators. Tappi J. 3(6):7-13.

Gasser, U., E.R. Weeks, A. Schofield, P.N. Pusey, and D.A. Weitz1. 2001. Real-space imaging of nucleation and growth in colloidal crystallization. Science. 292:258-262.

Khrenov, V., M. Klapper, M. Koch, and K. Müllen. 2005. Surface functionalized ZnO particles designed for the use in transparent nanocomposites. Macromol. Chem. Phys. 206(1):95–101.

Kocman, V. and P. Bruno. 1995. Accurate determination of six common fillers in fine papers, newsprint, and recycled stock by X-ray fluorescence spectrometry. Tappi J. 78(4): 129-134.

Kocman, V. and P.J. Bruno. 1996. Thermal stability of paper fillers: A strong case for a low temperature paper ashing. Tappi J. 79(3): 303-306.

Koepenick M. 2000. Nanoparticle prospects and perspectives. TAPPI J. 83(5): 45-47.

Kralj, D., J. Kontrec, L. Brečević, G. Falini, and V. Nöthig-Laslo. 2004. Effect of inorganic anions on the morphology and structure of magnesium calcite. Chem. Eur. J. 10:1647-1656.

Kuusipalo, J., M. Kaunisto, A. Laine, and M. Kellomäki. 2005. Chitosan as a coating additive in paper and paperboard. Tappi J. 4(8):17-21.

Kuang, D., A. Xu, Y. Fang, H. Ou, and H. Liu. 2002. Preparation of inorganic salts ($CaCO_3$, $BaCO_3$, $CaSO_4$) nanowires in the Triton X-100/cyclohexane/water reverse micelles. J. Crystal Growth 244:379–383.

Lee, S.Y., J. Lee, and S. Yang. 1999. Preparation of silica-based hybrid materials coated on polypropylene film. J. Materi. Sci. 34:1233-1241.

Lee, S.Y. 2002. Transcrystallization behavior and interfacial strength of a semicrystalline polymer combined with thermomechanical pulp (TMP) fiber. M.S. Thesis. Univ. of Idaho, Moscow, ID. 72 p.

Lee, S.Y., T.F. Shupe, L.H. Groom, and C.Y. Hse. 2006. Heterogeneous nucleation of a semicrystalline polymer on fiber surfaces. In: Recent developments in the particleboard, fiberboard, and molded wood products industry. Shupe, T.F. ed. Forest Products Society. Madison, WI. pp. 99-105.

Li, L., A. Collis, and R. Pelton. 2002. A new analysis of filler effects on paper strength. JPPS. 28(8):267-273.

Lork, A. 2004. Silicone resin emulsion coatings: the strength profile of the silicone resin network in paint microstructures. Surface Coatings Inter. Part B: Coatings Transa. 87(B1):1–6.

Ma, C., M. Rong, M. Zhang, and K. Friedrich. 2005. Irradiation-induced surface graft polymerization onto calcium carbonate nanoparticles and its toughening effects on polypropylene composites. Polym. Engin. Sci. 45(4):529-538

Mullin, J.W. 1993. Crystallization, 3rd Ed. Butterworth-heinemann Ltd. Oxford, England. 527p.

Perng, Y. and E. Wang. 2004. Development of a functional filler: swelling sericite. Tappi J. 3(6):26-31.

Perng, Y. and E. Wang. 2004. Development of a functional filler: swelling sericite. Tappi J. 3(6):26-31.

Sancaktar, E., and E. Walker. 2004. Effects of calcium carbonate, talc, mica, and glass-fiber fillers on the ultrasonic weld strength of polypropylene. J. Appli. Polym. Sci. 94:1986–1998.

Tappi. 1993. Tappi test method T211 om-93 Ash in wood, pulp, paper and paperboard: combustion at 525°C. Tappi. Atlanta, GA.

Yan, Z., Q. Liu, Y. Deng, and A. Ragauskas. 2005. Improvement of paper strength with starch modified clay. J. Appl. Polym. Sci. 97: 44–50.

Advanced Biomass Science and Technology for Bio-Based Products

Editors
Chung-Yun Hse, Zehui Jiang, and Mon-Lin Kuo

Associate Editors
Feng Fu and Paul Y. Burns

Developed from a symposium sponsored by:
Chinese Academy of Forestry & USDA Forest Service, Southern Research Station

May 23-25, 2007
Beijing, China